Verification of seismic performance of an isolated bridge subjected to the 2011 off the Pacific coast of Tohoku earthquake

G. Shoji

Faculty of Engineering, Information and Systems, University of Tsukuba, Tsukuba, Japan.

M. Fujikawa

East Japan Railway Company Tokyo Construction Office, Tokyo, Japan.

ABSTRACT: Seismic performance of an isolated bridge subjected to the 2011 off the Pacific coast of Tohoku earthquake was verified by analysing observed acceleration waveforms at the girders, piers, foundation and ground surface. Typical isolated bridge with the fundamental natural period of more than about 1.0 s located at a waterfront of Tokyo Bay was selected for analysis. Values of equivalent stiffness and damping ratio for isolators installed in the bridge were identified by analysing the transfer functions computed by the data of Fourier transforms for observed response data at the girder on P4 pier and P4 pier top. Uncertainty of identified values of the equivalent stiffness and damping ratio was quantitatively determined by using Bootstrap sampling. Seismic responses of the bridge were clarified by comparing the observed responses and simulated ones from nonlinear dynamic analysis based on three dimensional frame structural model by using the values of identified equivalent stiffness and damping ratio of isolators.

1 INTRODUCTION

Infrastructures were severely suffered by induced ground motions as well as by tsunami waves during the 2011 off the Pacific coast of Tohoku earthquake (hereinafter, the 2011 Tohoku earthquake). Long-period ground motions (hereinafter, LGMs) were induced at the plains and basins in Tohoku and Kanto areas. The LGMs might excite long-period infrastructure such as long viaducts and energy liquid tanks. Isolated bridges and long-span bridges are also classified into long-period infrastructure. Hence, it is significant to analyze the response data observed at an isolated bridge subjected to LGMs.

Yoshida et al. (1999) identified the dynamic characteristics of isolators on Matsunohama elevated highway bridge in Hanshin expressway by analyzing observed data during the 1995 Kobe earthquake, which is an inland-shallow earthquake. Kaito et al. (1999) proposed the method for evaluating structural performance of bridges with considering the uncertainty by using observed dynamic response data, and they applied the method to system identification for Yama-age isolated bridge. As well as these researches, seismic performance of isolated bridges subjected to extreme ground motions was examined by analyzing the observed data (for instance, Chaudhary et al. 2002, Ina et al. 2008). However, system identification of isolated bridges subjected to LGMs has not been sufficiently done because huge plate boundary and inner plate earthquakes have not been frequent for exposing an isolated bridge.

Therefore, we verify seismic performance of a typical isolated bridge with the fundamental natural period of more than 1.0 s located at a waterfront of Tokyo Bay subjected to extreme ground motions observed in the 2011 Tohoku earthquake by carrying out nonlinear dynamic response analysis. The stiffness and damping coefficient of isolators installed in the bridge are identified by analyzing the transfer functions for observed response data of girders and pier top. Seismic responses of the bridge are clarified by comparing the simulated responses and observed ones by using identified equivalent stiffness and damping ratio of isolators.

2 SUBJECT ISOLATED BRIDGE AND OBSERVED RESPONSE DATA

2.1 Higashi-ohgishima isolated bridge

Table 1 shows the characteristics of subject isolated bridge. Figure 1 shows the side view and location of accelerometers. Subject bridge is the Higashi-ohgishima viaduct consisting of 9-span decks by prestressed concrete (PC) box girders with 2 isolators on each pier, 8 wall-type piers and 2 abutments, and supported by steel-pile foundations (Nakagawa 1994). Structural type of an isolator is a lead rubber bearing (LRB). An isolator can move freely in longitudinal direction (LG) and the motion of an isolator is limited in transverse direction (TR) by side blocks, which function to prevent transverse motion of girders. Table 2 shows characteristics of isolators. Subjected bridge is located on reclaimed land at a waterfront of Tokyo Bay, which is classified into Type 3 ground condition by Design Specifications for Highway Bridges (2012).

Table 1. Characteristics of Higashi-ohgishima isolated bridge.

Total length	417.6[m] (8×45.0[m]+55.0[m])
Effective width of deck	14.25[m]
Superstructure	9-span PC box girders
Substructure	2 abutments, 8 wall-type piers
Foundation	8 steel pipes with diameter of 0.8[m], and length of 40.0[m] (P4)
Isolator	2 lead rubber bearings (LRBs) on each pier
Ground condition	Type 3 in Design Specifications for Highway Bridges (2012)

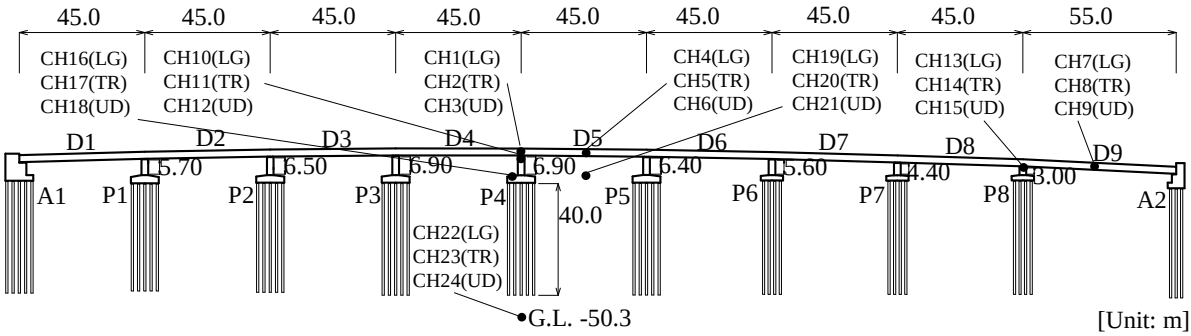

Figure 1. Side view of the isolated bridge and location of accelerometers.

Table 2. Characteristics of isolators.

Area [m^2]	1.23[m]×1.80[m]=2.21
Shear modulus of rubber G [MN/m^2]	0.98
Thickness of rubber [m]	0.036[m]×5 layers=0.18
Area of lead plugs A_p [m^2]	Diameter of 0.02[m]×4 plugs, A_p=0.126
Effective area to an axial pressure A_R [m^2]	2.09
1st shape factor S	9.57
Compressive stiffness K_V [MN/m]	68.97
Lateral stiffness K_R [MN/m]	11.38
Yielding load of lead plugs Q_d [MN]	1.05

2.2 Observed seismic response data

During the 2011 Tohoku earthquake, acceleration waveforms were observed at the center of D5 and D9, at the girder on P4, on the P4 and P8 tops, on the P4 footing, in the ground of -50.3 m under the ground surface, and on the ground surface between P4 and P5. Each seismometer records the LG, TR and UD components as shown in Figure 1. Figure 2 shows acceleration waveforms without filtering observed at the girder on P4, on the P4 top, and on the ground surface between P4 and P5. Figure 3

shows spatial distribution of corresponding maximum absolute accelerations. In addition, Figure 4 shows acceleration response spectra with damping ratio of 0.05 computed by using the observed acceleration data on the ground surface. Figure 4 also shows the design spectrum for Level 2 Type 1 and Type 2 ground motions in Type 3 ground condition described by Design Specifications for Highway Bridges (2012). From Figures 2 to 4, the maximum response acceleration at the girder on P4 in LG direction is about half than that in TR direction. This indicates that the response at the girder on P4 in LG direction is reduced by elongating the natural period of the bridge by installation of isolators on the P4 top.

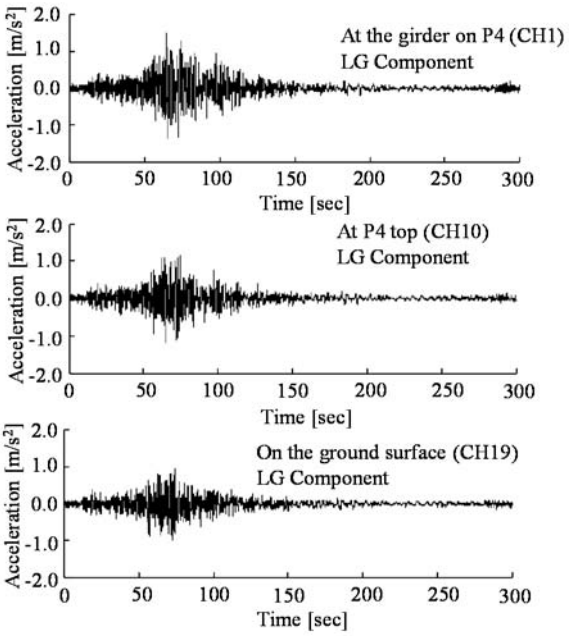

Figure 2. Observed acceleration waveforms.

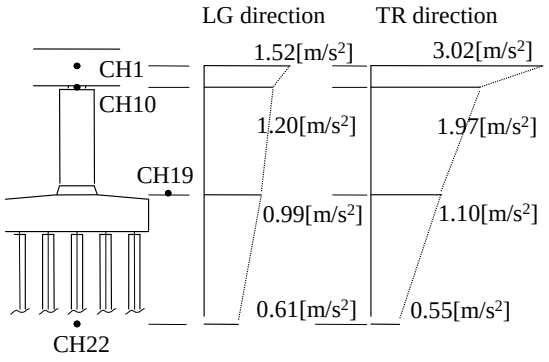

Figure 3. Maximum absolute accelerations at P4.

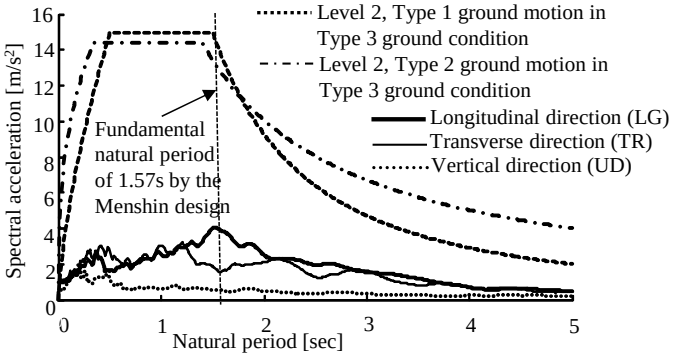

Figure 4. Acceleration response spectra with damping ratio of 0.05.

3 IDENTIFICATION OF DYNAMIC CHARACTERISTICS OF ISOLATORS

3.1 Identification of dynamic characteristics

Natural frequency f_0 Hz and damping ratio ς of isolators on the P4 top in LG direction were identified by analysing the transfer functions computed by Fourier transforms for observed response data of the girder on P4 and the P4 top based on modelling of the single degree of freedom system. When computing the Fourier transforms, the acceleration data were filtered out by a 10 Hz low-pass filter. The equation of motion is given by

$$\ddot{x} + 2\varsigma\omega_0\dot{x} + \omega_0^2 x = -\ddot{y} \tag{1}$$

in which x is the relative displacement of the girder on P4 to the P4 top, y is the relative displacement of the P4 top to the ground surface, ω_0 is the natural angular frequency of isolators and ς is the damping ratio. $f_0 = \omega_0 / 2\pi$. Transfer function $H(f)$ of $\ddot{x}$ compared with $\ddot{y}$ in Equation 1 is computed theoretically as below.

$$H(f) = \frac{f^2}{-f^2 + 2i\varsigma \cdot f_0 f + {f_0}^2} \tag{2}$$

in which f is the frequency of y with harmonic excitation and i is the imaginary unit.

For computing the transfer function $\bar{H}(f)$ for observed acceleration data, the data is divided into N sub-data sets which have statistical decorrelation each other with autocorrelation coefficient of less than 0.2. Each sub-data set has S data. In the following computation, N =19 sub-data sets are generated with S =1,024 data by permitting the overlap data of $S/2$ =512 between two sub-data sets. For each sub-data set, the j th frequency is defined as below.

$$f_j = \frac{j}{S \cdot \Delta t} \tag{3}$$

Here, Δt is the time interval of data and Δt =0.01 s for observed data. For n th sub-data set, the transfer function $\bar{H}(f_j)$ is computed by using the Fourier transforms $F_{\ddot{x}}^n(f_j)$, $F_{\ddot{y}}^n(f_j)$ and the complex conjugate $F_{\ddot{y}}^n(f_j)^*$ for acceleration data $\ddot{x}$ and $\ddot{y}$ as below.

$$\bar{H}(f_j) = \frac{\sum_{n=1}^{N} \left| F_{\ddot{x}}^n(f_j) \cdot F_{\ddot{y}}^n(f_j)^* \right|}{\sum_{n=1}^{N} \left| F_{\ddot{y}}^n(f_j) \right|^2} \tag{4a}$$

Based on Bootstrap sampling method, B =2,000 samples of $F_{\ddot{x}}^n(f_j)$ and $F_{\ddot{y}}^n(f_j)$ are generated by using pseudorandom numbers and for b th sample the transfer function $\bar{H}^b(f_j)$ is computed as below.

$$\bar{H}^b(f_j) = \frac{\sum_{n=1}^{N} \left| F_{\ddot{x}}^{b|n}(f_j) \cdot F_{\ddot{y}}^{b|n}(f_j)^* \right|}{\sum_{n=1}^{N} \left| F_{\ddot{y}}^{b|n}(f_j) \right|^2} \tag{4b}$$

For b th sample natural frequency f_0^b and damping ratio ς^b of isolators on the P4 are calculated by minimizing the value evaluated in the frequency domain from the lower limit f_{jl} =0.49 Hz corresponding to the number of frequency order j_l =5 to the upper limit f_{ju} =4.98 Hz corresponding to the number of frequency order j_u =51 by the function E defined as below.

$$\begin{aligned} E = \frac{1}{2f_j} \Bigg[& \left\{ \left| H(f_{j_l}) \right| - \left| \bar{H}^b(f_{j_l}) \right| \right\}^2 + 2 \sum_{j=j_l+1}^{j_u-1} \left\{ \left| H(f_i) \right| - \left| \bar{H}^b(f_i) \right| \right\}^2 \\ & + \left\{ \left| H(f_{j_u}) \right| - \left| \bar{H}^b(f_{j_u}) \right| \right\}^2 \Bigg] \end{aligned} \tag{5}$$

From B =2,000 samples, finally, the expected value μ_{f_0} and μ_ς, standard deviation σ_{f_0} and σ_ς for natural frequency f_0 and damping ratio ς of isolators were identified with showing 99% confidence level in Figure 5.

3.2 **Model of isolators**

Expected value μ_{K_e} of equivalent stiffness K_e of isolators on the P4 was idealized by the following equation.

$$\mu_{K_e} = 4\pi^2 m \mu_{f_0}{}^2 \quad (6)$$

In Equation 6 m is the mass supported by isolators on the P4 and $m = 7.71$ MN was determined by the associated design documents. By μ_{f_0} =1.358 Hz in Equation 6, μ_{K_e} was calculated to be 56.07 MN/m. Figure 6 shows the hysteresis loop of isolators for observed data and identified equivalent stiffness μ_{K_e} . K_e has the smaller value compared with the observed hysteresis loop, while the isolators response linearly within about 80% to 90% range of yielding load of lead plugs Q_d (Table 2).

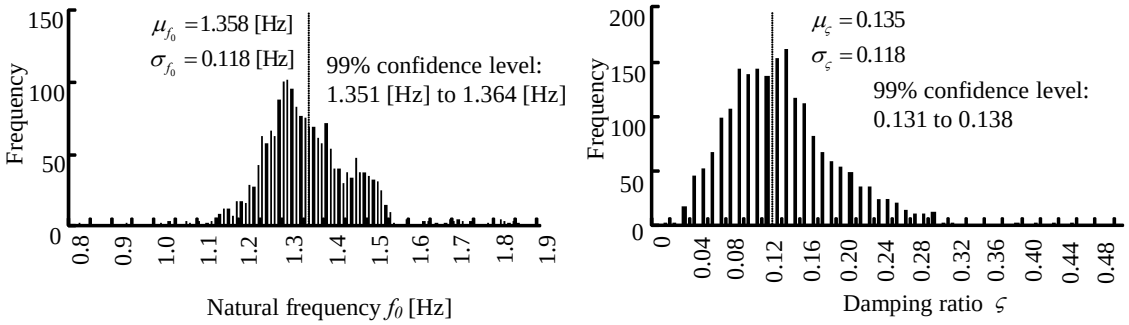

Figure 5. Histograms for identified natural frequency f_0 and damping ratio ς of isolators on the P4.

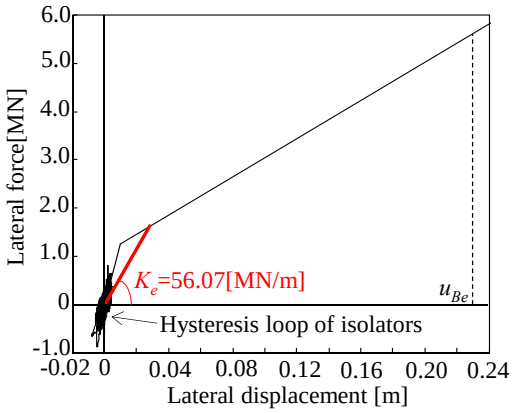

Figure 6. Hysteresis loop of isolators on the P4 for observed data and identified equivalent stiffness K_e.

4 SEISMIC RESPONSE ANAYSIS BY USING MODEL PARAMETERS

4.1 Analytical model

Nonlinear dynamic analysis was done to verify the values of identified model parameters of isolators on the P4 by using three-dimensional frame model shown as Figure 7. The deck and girder were idealized as a linear beam element. The Young's modulus was set to be 2.45×10^4 MN/m^2 and elastic shear modulus to be 1.07×10^4 MN/m^2. The skeleton curve for inelastic hinge of each pier bottom was modelled by tri-linear model to take into account of material nonlinearity: cracking, yielding and ultimate points. The internal curve of pier hysteresis was modelled by Takeda model considering the degradation of the stiffness (Takeda et al. 1970). Sway, rocking and their coupled springs describing the interrelated motion of pile foundations and ground property were attached at the bottom of each footing.

The modal properties for the bridge model were determined by eigenvalue analysis based on above model. The dominant mode in LG direction is the fundamental mode with natural period of 1.06 s, showing the horizontal sway mode of decks and girders supported by isolators. The dominant modes in TR direction are the 2nd and 4th ones with natural period of 0.97 s and 0.64 s, showing symmetric bending vibration mode of decks and girders. For UD direction, 5th and 17th modes are dominant

showing the longitudinal vibration modes of decks and girders. The ratio of effective mass to total mass for fundamental and 2nd modes become over 68% in LG direction and over 44% in TR direction.

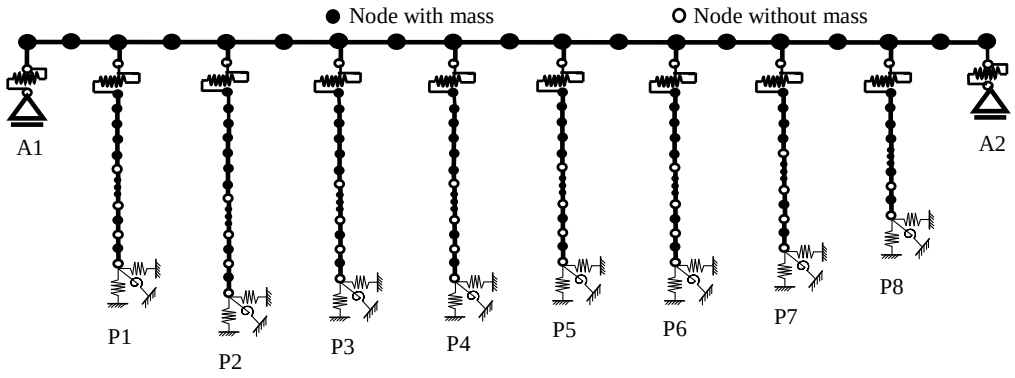

Figure 7. Analytical frame model.

The Newmark β scheme was used for numerical integration with an integral increment of 0.01 s. Viscous damping ratios for deck and girders, pier, and foundation were assumed to be 0.02, 0.02 and 0.20. The damping ratio for isolators on all piers was set to be 0.135 by using μ_ς in Section 3. The damping matrix in the equation of motion was modelled by Rayleigh damping with two constant coefficients of α_0 =0.359 and α_1 =0.011 determined by natural frequencies and modal damping ratios for fundamental and 20th modes.

4.2 Comparison of simulated waveforms with observed waveforms

Figure 8 show acceleration responses of the girder on P4 and the P4 top. Figure 9 show the corresponding Fourier spectra. In terms of these comparisons, the acceleration waveforms were filtered out by a 10 Hz low-pass filter.

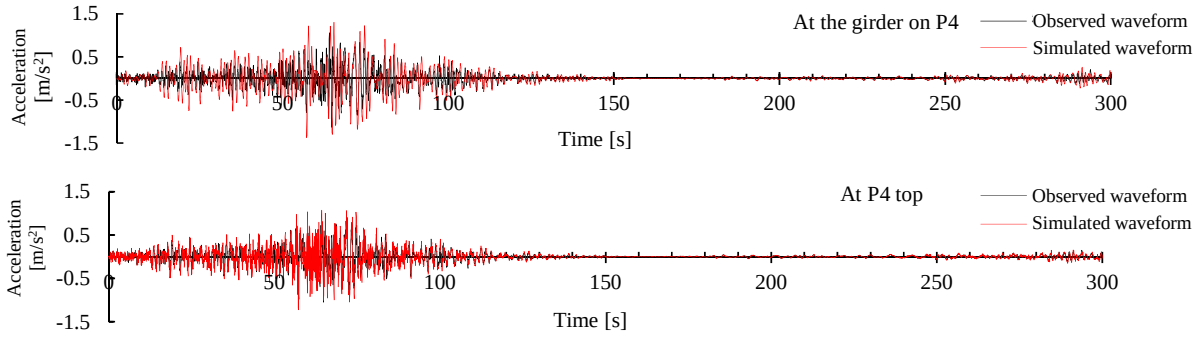

Figure 8. Acceleration responses.

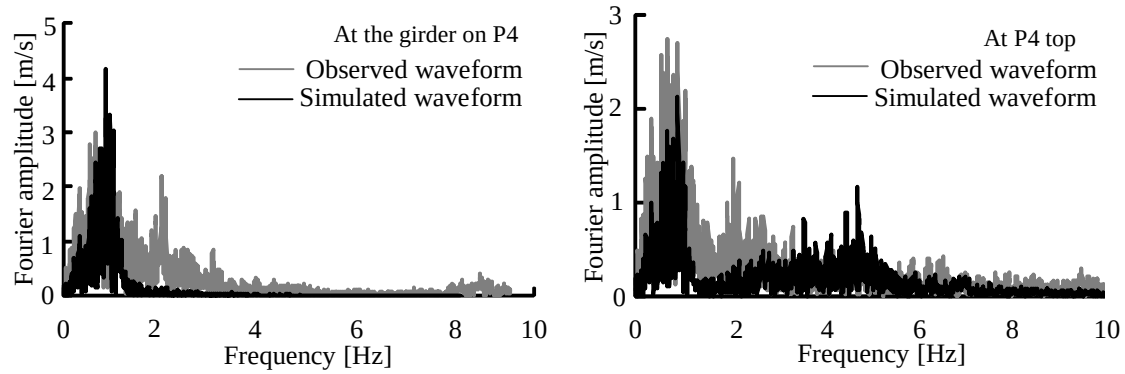

Figure 9. Fourier spectra for acceleration responses.

From Figure 8 the simulated waveform at the girder on P4 gives good agreement with observed one, whereas maximum acceleration of 1.37 m/s^2 for simulated waveform is slightly different from that of 1.13 m/s^2 for observed waveform. Moving onto the comparison of simulated and observed waveforms at P4 top, the general trend is approximately same as that for the girder on P4, showing maximum acceleration of 1.23 m/s^2 for simulated waveform and of 1.05 m/s^2 for observed waveform.

From Figure 9 the dominant frequencies of Fourier spectra for simulated and observed waveforms at the girder on P4 show exactly same value of 0.90 Hz. The dominant frequency for simulated waveform at P4 top also shows at 0.90 Hz whereas that for observed waveform varies at 0.67 to 0.90 Hz. This frequency of about 0.90 Hz corresponds to the fundamental natural frequency of lateral sway motion in LG direction of decks and girders supported by isolators. Observed Fourier spectrum at the girder also shows peaks at frequencies of 2.08 Hz and 3.17 Hz. In contrast, simulated Fourier spectrum does not have peaks over 1.0 Hz frequency. Hence, the analytical model could not simulate higher modal properties of the bridge in LG direction due to the vibration of pier, footing and foundation because of the possibility of inappropriately modelling of seismic strengthening at the plastic-hinge region of a pier.

5 **CONCLUSION**

Seismic performance of an isolated bridge subjected to the 2011 off the Pacific coast of Tohoku earthquake was verified by analysing observed acceleration waveforms at the girders, piers, foundations and ground surface. Typical isolated bridge with the fundamental natural period of more than about 1.0 s located at a waterfront of Tokyo Bay was selected for analysis.

First, expected values of equivalent stiffness K_e and damping ratio ς for isolators on P4 pier of the bridge were identified to be μ_{K_e} =56.07 MN/m and μ_{ς} =0.135 by analysing the transfer functions computed by Fourier transforms for observed response data at the girder on P4 and the P4 top. Uncertainty of identified equivalent stiffness and damping ratio was quantitatively determined by showing the 99% confidence level by using Bootstrap samples.

Seismic responses of the bridge were clarified by comparing the observed responses and simulated ones from nonlinear dynamic analysis based on three dimensional frame structural model by using the values of identified equivalent stiffness and damping ratio of isolators on P4. Simulated waveforms at the girder on P4 and the P4 top give good agreement with observed ones and dominant frequencies of Fourier spectra for simulated and observed waveforms at the girder on P4 and P4 top show approximately same value of 0.90 Hz, which suggests that this frequency corresponds to the fundamental natural frequency of lateral sway motion in LG direction of decks and girders supported by isolators for the isolated bridge.

ACKNOWLEDGMENTS:

The authors are most grateful to Metropolitan Expressway Company Limited for the invaluable cooperation in providing acceleration response data at Higashi-ohgishima isolated bridge recorded in the 2011 off the Pacific coast of Tohoku earthquake.

REFERENCES:

Chaudhary M.T.A., Abe M. & Fujino Y. 2002. Investigation of atypical seismic response of a base-isolated bridge. *Engineering Structures*, 24, 945-953.

Ina Y., Nakatani Y. & Kikuchi T. 2008. Earthquake behavior for PC road bridge using seismic-isolated bearing, *Journal of Japan Society of Civil Engineers A*, 64(4), 778-788.

Japan Road Association 2012. *Design specifications for highway bridges*, Part V.

Kaito K., Abe M. & Fujino Y. 1999. Performance evaluation of non-proportionally damped structures considering uncertainty, *Journal of Structural Engineering*, Japan Society of Civil Engineers, 45, 701-712.

Nakagawa M. 1994. Longest PC quake-free multispan continuous girder bridge (the East Ohgishima viaduct - tentative name) in Japan, Bridge, 30(9), 4-9.

Takeda T., Sozen M.A. & Nielsen N.N. 1970. Reinforced concrete response to simulated earthquakes, *Journal of Structural Division*, ASCE, 96(12), 2557-2573.

Yoshida J., Abe M. & Fujino Y. 1999. Performance of base-isolated bridge during 1995 Kobe earthquake based on observed record, *Structural Eng./Earthquake Eng.*, Japan Society of Civil Engineers, 626(I-48), 37-50.